Climate Dynamics (2026) 64:79
https://doi.org/10.1007/s00382-026-08081-8

The southern annular mode and its relationship with Antarctic temperature in contrasting future storylines

Gareth J. Marshall[1] · Ryan S. Williams[1] · Lise S. Graff[2] · Dörthe Handorf[3] · Alexey Y. Karpechko[4] · Raphael H. Köhler[3] · Xavier Levine[5] · Andrew Orr[1] · Priscilla A. Mooney[6]

Received: 10 June 2025 / Accepted: 13 January 2026

Abstract
The Southern Annular Mode (SAM) strongly modulates Antarctic near-surface air temperature (SAT) variability. We employ a storyline approach to examine projected end of century changes in the spatial SAM-SAT relationship across Antarctica in two models from the sixth phase of the Coupled Model Intercomparison Project (CMIP6) under a high end forcing Shared Socioeconomic Pathway (SSP5-8.5) for both austral winter and summer. The models represent a pair of climate storylines (termed B and C as in previous work) corresponding to plausible future physical changes in two remote drivers. Relative to the CMIP6 multi-model mean response, Storyline B is characterised by high seasonal sea ice extent loss and either low stratospheric polar vortex (SPV) strengthening in winter or early SPV breakdown in summer: Storyline C is distinguished by opposing projected changes. Our analysis demonstrates that deviations in the future SAM-SAT relationship are markedly greater between the two storylines in summer, when significant differences occur across much of Antarctica, than in winter. The greater differences in summer arise because Storyline B exhibits a less positive (more negative) relationship between the SAM and SAT across the Antarctic Peninsula (West Antarctica), in contrast to a less negative SAM-SAT relationship in East Antarctica: opposing changes are observed for Storyline C. Disparities in the former regions can be traced to differences in the location and strength of the climatological Amundsen Sea Low. This work highlights the use of the storyline approach to establish the spread of credible regional Antarctic climate responses across a single climate change scenario.

Keywords Southern annular mode · Antarctica · Climate · Storylines · Temperature · Projections

1 Introduction

The Southern Annular Mode (SAM) is the principal mode of extra-tropical Southern Hemisphere (SH) atmospheric circulation variability (see Fogt and Marshall (2020) for a review). The SAM is primarily a measure of the meridional pressure gradient between the mid and high SH latitudes and hence can be linked to changes in the properties of the circumpolar jet and associated westerly winds around Antarctica. The polarity of the SAM is defined as positive (SAM+) when pressure anomalies are positive (negative) at mid- (high-) latitudes and vice versa for the negative polarity (SAM−). SAM+ is generally characterised by a poleward shift and intensification of the jet, with SAM− having opposite characteristics. While the SAM structure is predominantly zonally symmetric, there is nevertheless a marked asymmetric component. In the troposphere this asymmetry comprises a zonal wave 3 pattern that is especially strong

✉ Gareth J. Marshall
gjma@bas.ac.uk

1 British Antarctic Survey, UK Research and Innovation, Cambridge, UK

2 Norwegian Meteorological Institute, Oslo, Norway

3 Helmholz Centre for Polar and Marine Research, Alfred Wegener Institute, Potsdam, Germany

4 Finnish Meteorological Institute, Helsinki, Finland

5 Columbia University, New York, USA

6 NORCE Norwegian Research Centre, Bjerknes Centre for Climate Research, Bergen, Norway

Published online: 03 February 2026

in the South Pacific (Campitelli et al. 2021), which is the region of the climatological Amundsen Sea Low (ASL) (e.g., Raphael et al. 2016). Changes in the strength and position of the ASL are a major driver of climate variability in West Antarctica and the Antarctic Peninsula (Hosking et al. 2013) (see Fig. 1a for place names used in the text). The ASL is the primary circulation pattern through which low frequency modes of variability in tropical sea surface temperatures (SSTs), such as the El Niño-Southern Oscillation (ENSO), Interdecadal Pacific Oscillation (IPO) and Atlantic Multidecadal Oscillation (AMO), impact interdecadal Antarctic climate variability (e.g., Clem et al. 2016; Li et al. 2021; Zhang et al. 2023; Sui et al. 2024). These tropical signals are communicated via the Pacific South American (PSA) atmospheric teleconnection pattern, which has the ASL as one of its primary centres of action (e.g., Marshall and Thompson 2016).

Changes in SAM polarity have a marked impact on near-surface temperature (SAT) anomalies across much of Antarctica. Thompson and Solomon (2002) were the first to describe the typical pattern of SAM+ being broadly concomitant with positive SAT anomalies over the Antarctic Peninsula and negative SAT anomalies over the remainder of the Antarctic continent. Subsequently, there has been much further work on SAM-SAT relationships in Antarctica (e.g., Marshall 2007; Marshall and Thompson 2016; Wachter et al. 2020). This 'standard' SAM-SAT pattern results from the interaction between the local Antarctic orography and the regional circulation. The Peninsula extends northwards into the circumpolar westerlies and the climate on its western side is often affected by winds associated with the ASL, which may have an amplified northerly or southerly component during SAM+, depending on its position. Furthermore, the stronger westerly jet impinging on the Peninsula is more likely to push air masses over the mountainous orography, leading to downslope föhn winds on the eastern Peninsula that can contribute to dramatic local SAT increases (e.g., Gilbert et al. 2022; Zou et al. 2023). Across the Plateau and East Antarctic coastal regions, the stronger circumpolar westerlies accompanying SAM+ isolate the continent from warmer mid-latitude maritime air masses so that SAT anomalies are predominantly negative (e.g., Marshall and Thompson 2016). Moreover, SAM+ is also associated with weaker katabatic drainage over East Antarctica, leading to stronger temperature inversions and thus lower SAT (van den Broeke and van Lipzig 2003).

However, a number of studies have described temporal variations in the Antarctic SAM-SAT relationship that deviate from the 'standard' pattern described above. At sub-decadal timescales these are primarily associated with changes in the non-annular component of the SAM (e.g., Marshall et al. 2013; Wachter et al. 2020), especially the phase and/or magnitude of the zonal wave 3 pattern. Such changes have been linked to variations in tropical convection (Goyal et al. 2021a) or associated with the large-scale patterns of tropical SST variability described previously (Wachter et al. 2020). The resultant changes in the SAM-SAT pattern tend to be regional: for example, Marshall et al. (2013) described a reversal from a negative to positive SAM-SAT relationship across East Antarctica in austral summer and autumn in the first decade of the 21st Century, which the authors suggested was likely due to internal

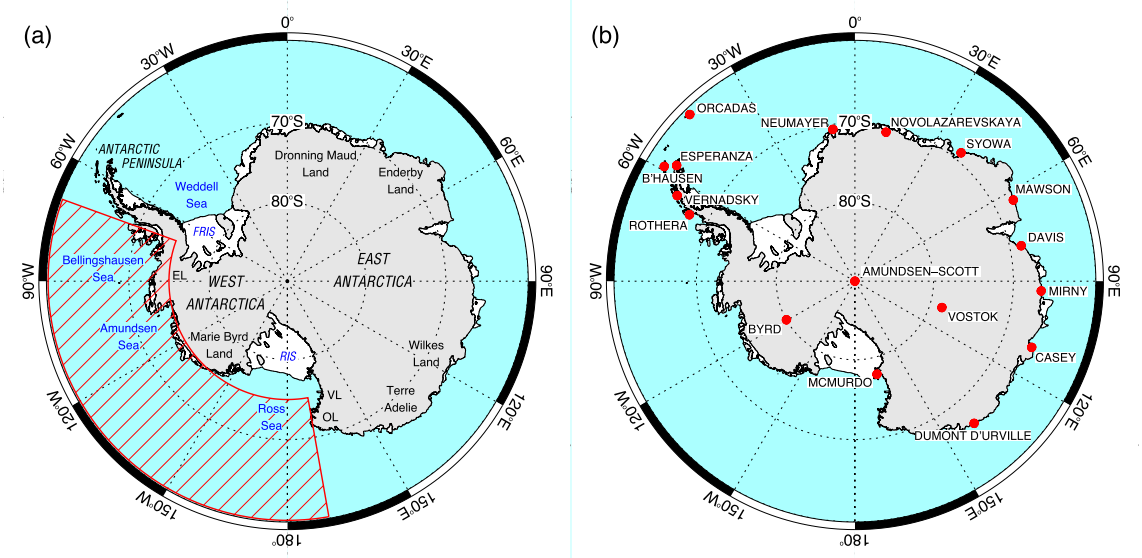

Fig. 1 Maps of Antarctica showing **a** the location of regions mentioned in the text. EL is Ellsworth Land, FRIS is Filchner–Ronne Ice Shelf, OL is Oates Land, RIS is Ross Ice Shelf and VL is Victoria Land. The shaded box outlined in red demarcates the region (ocean only) in which the ASL is defined as the SLP minima (see Sect. 2.7) **b** the location of the 17 Antarctic meteorological stations providing SAT observations for validation

climate variability. In addition, observations also suggest a more widespread reversal in the sign of the SAM-SAT relationship across Antarctica and elsewhere in the SH high latitudes that occurred around 1980 (Silvestri and Vera 2009; Fogt et al. 2012; Marshall et al. 2022). Antarctic stratospheric ozone depletion began about this time and is predominantly responsible for recent positive trends in the SAM during austral summer (e.g., Polvani et al. 2011; Thompson et al. 2011; Orr et al. 2012), so this process may be similarly accountable for the contemporaneous change in the spatial SAM-SAT pattern. Marshall et al. (2022) examined changes in SAM structure associated with this shift in the SAM-SAT pattern and demonstrated that in the more recent period the SAM became less zonal and, in particular, the magnitude of the zonal wave 3 pattern increased together with an eastward shift in its phase. In the Peninsula region this manifested as a switch in the meridional wind component associated with SAM+ from southerly to northerly as the ASL shifted east, closer to the region. Given that SAM variability has significant implications for Antarctic surface melt, including those regions with ice shelves that are critical in maintaining the stability of the Antarctic Ice Sheet (e.g., Gilbert et al. 2022; Orr et al. 2023; Saunderson et al. 2024), it is important to examine how SAM structure and its influence on the SAM-SAT relationship may change in the future.

The most recent suite of model experiments from the sixth Coupled Model Intercomparison Project (CMIP6; Eyring et al. 2016; see Sect. 2.2), as employed in the Intergovernmental Panel on Climate Change (IPCC) sixth assessment report (IPCC 2023), have been shown to be better at reproducing recent SH climate than their predecessors in CMIP5 (Taylor et al. 2012), having a significant reduction in the equatorward bias of the subtropical jet (i.e. a too negative SAM) (e.g., Bracegirdle et al. 2020; Goyal et al. 2021b). Moreover, Coburn and Pryor (2021) concluded that all CMIP6 models exhibited the basic spatial structure of the SAM, although in several the high latitude contribution was too great, with an intensified belt of circumpolar westerlies around Antarctica. Similarly, Zhang et al. (2022) determined that the asymmetrical component of the SAM was key to correctly reproducing overall SAM structure in CMIP6. This corroborates the findings of Marshall and Bracegirdle (2015), that the ability of the earlier CMIP5 models to replicate observed Antarctic SAM-SAT relationships was compromised by their inability to provide an accurate facsimile of regional meridional flow. The capability of CMIP6 models to represent Antarctic SAT has been shown to vary widely between models and often in previous studies only a subset of the best performing models were selected for analysis (e.g., Tewari et al. 2022).

The direction of future changes in the summer SAM have long been thought of as a 'tug of war' between 21st Century stratospheric ozone recovery and greenhouse gas (GHG) forcing, pushing the SAM towards a more negative and positive polarity, respectively (e.g., Arblaster et al. 2011; Thompson et al. 2011; Simpkins and Karpechko 2012). In future CMIP6 projections, the SAM experiences divergent changes dependent on which of the Shared Socioeconomic Pathway (SSP) scenarios that comprise the Scenario Model Intercomparison Project component of CMIP6 (O' Neill et al. 2016) is used. In SSP1-2.6, a low-end forcing pathway, the mean SAM polarity remains similar or becomes more negative across the remainder of the 21st Century as stratospheric ozone recovers. In contrast, in SSPs with greater forcing, the SAM generally becomes more positive with the strongest trends in austral autumn and weakest in winter (Deng et al. 2022). However, we note that the relative seasonal strength of future changes in the SH westerlies is somewhat uncertain, with Goyal et al. (2021b) predicting the smallest increase in summer, as one might expect given predicted stratospheric ozone recovery and Deng et al. (2022) predicting the smallest change in winter (similar to the SAM). This marked difference in findings may result from the two studies utilising a different subset of CMIP6 models and, in particular, how the models used simulate stratospheric ozone depletion (see Keeble et al. 2021; Morgenstern 2021).

Projections of future climate are typically based on the multi-model mean (MME) of a large number (or ensemble) of coupled climate models. However, this approach is not necessarily the best estimate of future climate because individual models can deviate markedly from the MME and many climate models share common biases such that the MME should not be interpreted in a purely probabilistic sense (Knutti et al. 2013). Moreover, regional climate change within global climate models is inconsistent because of the dominant role of internal atmospheric circulation variability (Shepherd 2014): in the SH extra-tropics this uncertainty projects strongly onto the SAM (e.g., Deser et al. 2012). Conversely, in the climate storyline approach utilised here, inter-model diversity in the patterns of projected climate response is sampled by statistically constructing scenarios contingent upon the strength of the climate change signal of remote drivers (predictors) that impact the large-scale atmospheric circulation (e.g., Zappa and Shepherd 2017; see Sect. 2.1). These drivers are selected as known physical connections to the regional climate under examination and provide a best estimate of the regional response conditional on the response of the selected remote drivers to future changes in GHGs and other forcings. By considering n drivers, 2^n storylines can be generated with high/low values of each driver. Storylines therefore explicitly communicate uncertainty in future projections, and in this respect, differ from other approaches, such as emergent constraints

(e.g. Sun et al. 2025), which aim to construct a best projection by attempting to minimise the uncertainty.

The first SH climate storyline analysis was undertaken by Mindlin et al. (2020) using the earlier CMIP5 models under the Representative Concentration Pathway 8.5 (RCP8.5; van Vuuren et al. 2011). They constructed austral winter and summer storylines using the magnitude of tropical upper-tropospheric warming for each season and stratospheric polar vortex (SPV) variability—strengthening in winter and breakdown delay in late-spring/summer—as the remote drivers. More recently, Williams et al. (2024) undertook a similar analysis but utilised the updated CMIP6 models (SSP5-8.5) and with Antarctic sea-ice loss and SPV response as the two predictors—chosen because they have been shown to exert an influence on the SH extratropical atmospheric circulation (e.g., Ayres et al. 2022; Byrne et al. 2019) and contribute uncertainty to its future response in model simulations (Bracegirdle et al. 2018; Ceppi and Shepherd 2019)—yielding a higher explained variance in circulation response over parts of the high latitude Southern Ocean compared to the predictor combination of Mindlin et al. (2020). Both studies demonstrated that their selected drivers exert a marked response in the strength and/or position of the SH midlatitude jet stream. For example, Williams et al. (2024) found that a combination of the two drivers in their study explained 35% and 70% of the jet response in winter and summer, respectively. In addition, they noted that a strengthening of the jet is associated with reduced Antarctic surface warming whereas changes in jet position exerted a greater control on high-latitude precipitation. While both of the above changes in the kinematic properties of the jet can be linked to infer changes in the SAM, Mindlin et al. (2020) revealed that the regional circulation response in the SH extratropics was not zonally symmetric and thus not well represented by future modifications to the SAM.

In this paper we focus on the two storylines that were highlighted by Williams et al. (2024) for demonstrating the most contrast for dynamically sensitive variables. We use the CMIP6 models selected by Williams et al. (see Sect. S2) to best represent the winter and summer storylines to investigate how the relationship between the SAM and Antarctic SAT may change between the 'present' (1985–2014) and the 'future' (2070–2099), and how that specifically relates to changes in SAM structure. In Sect. 2, we describe the materials and methods used, including an overview of the climate storyline methodology. Results are provided for austral winter and summer separately, together with an analysis of the relationship between SAM structure and the ASL (Sect. 3). Finally, in Sect. 4 we summarise our key findings and discuss them in the context of potential regional impacts and the limitations of the storyline approach.

Table 1 Definition of the storylines used by Williams et al. (2024)

Storyline	Predictors
A	High SIE loss and strong SPV strengthening (late SPV breakdown)
B	High SIE loss and weak SPV strengthening (early SPV breakdown)
C	Low SIE loss and strong SPV strengthening (late SPV breakdown)
D	Low SIE loss and weak SPV strengthening (early SPV breakdown)

Summer SPV predictor in parentheses

2 Materials and methods

2.1 Storyline methodology

The details of the specific storyline methodology employed here are described in Williams et al. (2024) and summarised in the Supplementary Material Sect. S1. These storylines correspond to differences in two predictors shown to be uncorrelated across the models investigated: (i) the simulated amount of seasonal sea ice extent (SIE) loss and (ii) either (a) wintertime SPV strengthening or (b) the timing of the summertime SPV breakdown. The SPV response is fundamentally driven by the hemispheric meridional temperature gradient. This resulted in four storylines, labelled A–D (see Table 1). The four storylines can be considered as two pairs—A–D and B–C—with each member of a pair having an opposite future response in both the two predictors to the other. Austral winter and summer were defined as June-July–August and December-January–February-March, respectively: the extension of an extra summer month was to ensure the Antarctic sea-ice minimum, typically late February, would be fully captured. SPV strengthening was computed from mean zonal 50 hPa wind (U50) between 50 and 60°S for June-July–August and November–December for winter and summer, respectively.

In this study we contrast storyline pair B–C, in which the two models demonstrated greater differences between themselves relative to the present than storyline pair A–D in terms of a strengthened mid-latitude jet in both winter and summer and also a poleward shift in the latter season (Williams et al. 2024). This pair of storylines thus better explores the possible range of future changes in SH extratropical circulation.

2.2 CMIP6 model data

Williams et al. (2024) identified the CMIP6 models that best represented each storyline. These models were chosen based on (i) their capability to reproduce the predictors and additional variables in comparison to ERA5 during the present period, and (ii) their ability to represent the

relevant storyline in terms of equal weight between the two predictors. A summary of this methodology is provided in the Supplementary Material Sect. S2. Predictor values for each model were calculated and normalised against the model's'future warming', defined as the global annual mean temperature change between a historical baseline of 1940–69 and 2070–99. This stage removed any uncertainty due to 'global warming' from the atmospheric circulation response (Zappa and Shepherd 2017). The future climate projections were derived from SSP5-8.5, which symbolises the high end of the range of future pathways, forced by continued fossil-fuel driven development, and leads to a radiative forcing of 8.5 W m^{-2} by 2100 (O'Neill et al. 2016). The CMIP6 models chosen by Williams et al. (2024) to best represent storylines B and C in winter and summer are given in Table 2.

Monthly SAT and sea level pressure (SLP) data for the first model realisation (typically r1i1p1f1) of each of the selected CMIP6 storyline models were obtained from the historical runs for the present (1985–2014) and SSP5-8.5 projections for the future (2070–2099). Note that the present period was chosen as the final 30 years of the historical CMIP6 model runs.

Only three models were actually used as MPI-ESM1-2-LR best represents Storyline C in both winter and summer. A summary of these models and some of their key characteristics is provided in Table 2. All model data were interpolated to a 1.0 × 1.0° lat./lon. grid. We note the differing future warming values among the models (see Table 2). As this analysis is primarily exploring SAM structure and the SAM-SAT relationship via correlations then this is not considered highly important in this context: however, when considering actual SAT changes between the storyline models the results are normalised to the future warming in MPI-ESM1-LR. In addition, there is one selected model with interactive ozone but, as previous work does not reveal a clear consistent difference in total column ozone between models with and without interactive ozone, we do not discuss this issue further other than to note that Keeble et al. (2021) state that this model, CESM2-WACCM, has a lower total column ozone than their CMIP6 MME.

2.3 The European centre for medium-range weather forecasts (ECMWF) fifth generation reanalysis (ERA5)

ERA5 is the current ECMWF reanalysis and is described in Hersbach et al. (2020). It employs the Integrated Forecast System Earth System Model (cycle 41r2) and associated 4D-Variational assimilation scheme, as used in the 2016 ECMWF operational system. It has a spatial resolution of 31 km, 137 vertical levels to a 1 hPa pressure level, and output with a temporal resolution of 1 h. ERA5 comprises two distinct temporal components, from 1979 to present and a backward extension from 1940 to 1978 (Soci et al. 2024). In the more recent period, ERA5 Antarctic SAT generally corresponds closely to station observations and it is able to accurately reproduce the SAM (e.g., Gossart et al. 2019; Bozkurt et al. 2020; Zhu et al. 2021; Marshall et al. 2022; Bromwich et al. 2024). However, Soci et al. (2024) state that over the Southern Hemisphere for the early period the description of ERA5 seems mainly statistical. Although Marshall et al. (2022) suggested that ERA5 demonstrates some skill in reproducing both Antarctic SAT and the SAM pre-1979, in this analysis we limit the ERA5 data to the present (1985–2014). In addition, a recent study by King et al. (2022) demonstrated that ERA5 was able to accurately portray SLP variability over the Weddell Sea pack ice, indicating that the assimilation of satellite observations in this region is sufficient to enable it to reliably reproduce pressure over the Southern Ocean. SAT and SLP data were obtained on a 721 × 1440 lat./lon. grid.

2.4 SAT observations

In addition to using ERA5 to compare the SAM-SAT relationship in the models during the present period, we also utilise SAT observations from 17 Antarctic meteorological stations as a validation check on the former given that a few local discrepancies remain in the reanalysis (Bromwich et al. 2024). Note that these observations are indirectly assimilated into ERA5 via an offline SAT interpolation scheme. The stations are listed together with their coordinates and data availability for the present period in Table S1 and named on a location map (Fig. 1b). Monthly data were obtained from the

Table 2 Details of the three CMIP6 models used in this study

Model	Reference	Season/Storyline	Horizontal resolution	Ozone	Future warming
CAMS-CSM1-0	Rong et al. (2019)	Winter/B	160 × 320; 100 km	Prescribed	2.34 °C
MPI-ESM1-2-LR	Mauritsen et al. (2019)	Winter/C	96 × 192; 100 km	Prescribed	2.89 °C
CESM2-WACCM	Gettelman et al. (2019)	Summer/B	192 × 288; 100 km	Interactive	4.50 °C
MPI-ESM1-2-LR	Mauritsen et al. (2019)	Summer/C	96 × 192; 100 km	Prescribed	2.89 °C

Future warming is the difference in mean global near-surface temperature between the future (2070–2099) and present (1985–2014) under SSP5-8.5

quality-controlled READER (Reference Antarctic Data for Environmental Research) dataset (Turner et al. 2020), with the addition of the reconstructed SAT record from Byrd station in West Antarctica (Bromwich et al. 2013, 2014). Seasonal mean SAT values were only computed if data for all the relevant months were available.

2.5 Calculation of the SAM index

We employ a simple definition of the SAM taken from Gong and Wang (1999), which is calculated as the normalised zonal SLP anomaly at 40°S minus that at 65°S. Seasonal SLP fields are computed as the mean of the winter and summer months (JJA and DJFM), respectively. Seasonal zonal SLP is calculated as the average of 5° longitudinally spaced points around the 40°S and 65°S circles from these fields, with the mean and standard deviation derived for each latitude circle from the 30-year present (1985–2014). The seasonal SAM Index is then computed for each year for both present and future periods.

2.6 Calculation of SAM structure and associated zonal wave-numbers and relative meridional wind

We utilise zonal SAM-SLP correlation anomalies at 55°S as a summary diagnostic of SAM structure. This latitude typically lies between SAM-SLP correlations of opposite sign to the north and south, and therefore any anomalous changes in SAM structure will be manifested as fluctuations in correlations around this latitude circle (see Marshall et al. 2022 for details). In short, for every 5° longitude around 55°S the mean SAM-SLP correlation is derived as the mean of those from each of the 21 overlapping decades within the 30 years of data for a given storyline/time period/season combination and, subsequently, the anomalies calculated for each decade. In Fig. 4 the variability in zonal correlation anomalies is presented as the interquartile range derived from the 21 decades. To help quantify any differences in SAM structure, the zonal SAM-SLP correlation anomalies around the 55°S circle are decomposed into the first four zonal wave-numbers using Fourier analysis. As the SAM-SAT relationship across parts of Antarctica may be primarily determined by the regional meridional wind associated with the SAM polarity (Marshall and Thompson 2016; Wachter et al. 2020), we also estimate the mean meridional wind component and its relative magnitude associated with SAM+ for each storyline/period. This is computed by differentiating the SAM structure with respect to longitude, that is simply calculating the local change in the SAM-SLP correlation anomaly at 55°S (see Marshall et al. 2022).

2.7 Calculation of the relative depth and location of the Amundsen sea low (ASL)

As a key component of the SAM structure, we calculate the relative depth and location of the ASL. These parameters are computed using a methodology similar to Hosking et al. (2013). In brief, the ASL is defined as the SLP minima within a box bounded by 60–75°S and 170–290°E (see Fig. 1a) for grid cells that are considered as ocean in all three CMIP6 models. The relative depth of the ASL is subsequently calculated as the mean SLP within this box minus the ASL central pressure. Utilising relative depth as a measure of ASL strength rather than absolute SLP removes the broader SAM signal and allows a comparison between models with different background SLP climatologies. Occasionally secondary SLP minima occurred but the frequency of these was sufficiently low that the results were insensitive to them. For ASL location, we only assess changes in longitude as the latitude variability of the ASL is relatively small in the storyline models and, furthermore, previous work has shown that ASL latitude plays only a minor role in influencing Antarctic climate (Hosking et al. 2013).

2.8 Statistical methods

We employ the Wilcoxon signed-rank test to determine whether two populations are significantly different. The statistical significance of the SAM-SAT relationship at a point is calculated utilising the false discovery rate (*FDR*) methodology described by Wilks (2016), which accounts for spatial autocorrelation. Based on the recommendation for data that exhibit 'moderate to strong spatial correlation' in that paper, $\alpha_{FDR}=2\alpha_{global}$ where α is the significance level. To account for temporal autocorrelation in statistical analyses comparing the mean decadal SAM-SLP structure and zonal wave parameters between storyline models, the likely degrees of freedom in the data are estimated to be 1.5 times the number of non-overlapping decades (see Allen and Smith 1996).

3 Results

3.1 The relationship between the SAM and Antarctic temperatures

3.1.1 Winter

The CMIP6 models selected to represent Storylines B and C in winter are CAMS-CSM1-0 and MPI-ESM1-2-LR, respectively. (Table 2). Both these models have been shown to successfully capture the principal features of the SAM

while overestimating the variance explained by the SAM in SLP and geopotential height fields (Coburn and Pryor 2021; Nan et al. 2019). Thus, like the majority of CMIP6 models, the SAM structure is overall too zonal in both the models used for the winter storylines. Throughout Sect. 3.1.1 these models will simply be referred to as Storyline B and Storyline C, respectively.

The distribution of SAM values is shown in Fig. 2a for the present and future periods, based on a normalisation period of the former. In the present, ERA5 is positively skewed, with a longer tail at the higher SAM values while Storylines B and C have SAM distributions that are negatively skewed and approximately neutral, respectively. In the future, SAM values in both storylines typically become more positive and the Storyline C population more negatively skewed. The populations of SAM values from the two storylines are statistically different from each other ($p<0.05$): unsurprisingly, Storyline C, associated with strong SPV strengthening, has a more positive future SAM than Storyline B.

In Fig. 3 we investigate the winter relationship between the SAM and Antarctic SAT using a series of correlation and correlation-difference plots. The latter is a useful indicator of the 'direction of travel' of the SAM-SAT relationships in a storyline model, even if the model does not correctly reproduce the SAM-SAT spatial pattern in the present. In the top row the present SAM-SAT correlations in the two storylines (Figs. 3a, b) are compared to ERA5 and observations (Fig. 3c). ERA5 has the 'standard' spatial pattern of SAM-SAT relationship described previously, that is a positive correlation over the Peninsula and negative correlation across much of the rest of the Antarctic continent (Fig. 3c), with the maximum magnitude of the SAM-SAT correlation (r_{max}) being >0.6 (< −0.5) for the Peninsula (East Antarctica). The majority of both regions have areas where the SAM-SAT relationship is statistically significant ($p<0.05$) and this is corroborated by the station observations. In contrast, we note the lack of a positive SAM-SAT relationship over the Peninsula in Storyline B (Fig. 3a) and, while there is an area of positive correlation in Storyline C (Fig. 3b), it is smaller in both spatial extent and magnitude than in ERA5 ($r_{max}<0.5$). In West Antarctica both storylines have small regions of significant negative SAM-SAT correlations, whereas ERA5 has areas with a positive relationship. However, both models do correctly represent the broad, predominantly statistically significant negative SAM-SAT relationship across East Antarctica.

In the future period, in both storylines the area of positive SAM-SAT relationship in the Peninsula region is much greater than the present (Fig. 3d, e). However, in Storyline C this region is predominantly confined to the area west of the Peninsula, encompassing the Amundsen–Bellingshausen Sea, (ABS). Over East Antarctica, the negative sign of the SAM-SAT relationship remains largely unchanged in both storylines, with a slightly greater area of the region having a significant relationship and with similar r_{max} values.

Figure 3f and g show the difference in SAM-SAT correlation between the future and present periods in Storylines B and C, respectively. In addition to the more positive relationship in the Peninsula, both storylines show that the magnitude of the negative SAM-SAT relationship across West Antarctica is reduced in the future. Another common feature is an area of enhanced negative correlation in Dronning Maud Land in East Antarctica: the area of significant change is both greater in extent and more significant in Storyline B.

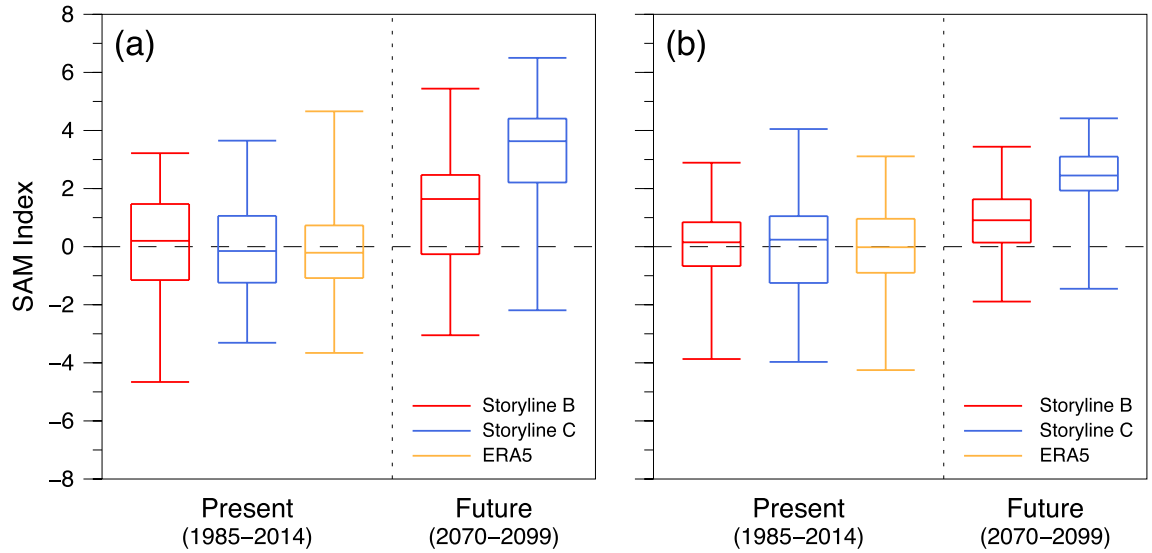

Fig. 2 The SAM calculated for the present and future periods based on the historical and SSP 5–8.5 projection, respectively, for winter (**a**) and summer (**b**). Storyline B is shown in red, Storyline C in blue and ERA5 in orange. The median, upper and lower quartiles (boxes) and range (whiskers) are shown. The SAM was normalised for the present (1985–2014) period

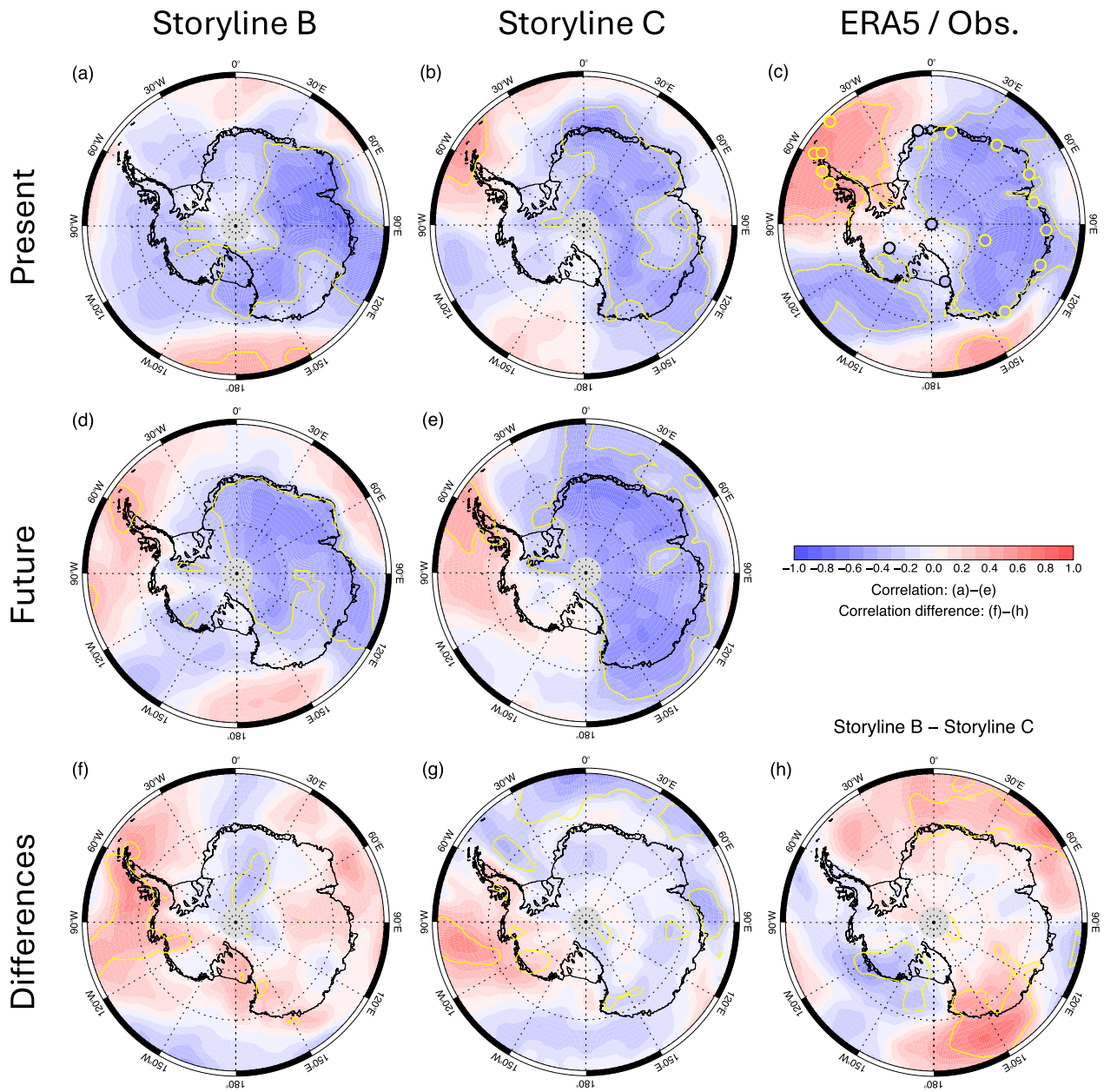

Fig. 3 Correlation between the SAM and SAT during winter for the present period: **a** Storyline B; **b** Storyline C; **c** ERA5; for the future period: **d** Storyline B; **e** Storyline C. Difference in SAM-SAT correlation values between future and present periods: **f** Storyline B; **g** Storyline C. **h** Difference between difference in correlations (Storyline B–Storyline C). Yellow contour in a–e represents a statistical significance of $p < 0.05$ calculated using the false discovery method. Similarly, in c, stations where the correlation is significant (not significant) at $p < 0.05$ are represented as yellow (black) circles, The grey circle represents missing data near the South Pole in one or more of the models

Thus, both storylines indicate a stronger dipole in the sign of the SAM-SAT relationship between the Peninsula and Dronning Maud Land than at present. Across the majority of the remainder of East Antarctica, the two storylines show opposite changes, with Storyline B having a more positive SAM-SAT relationship and Storyline C more negative, the latter demonstrating an enhanced version of the standard spatial SAM-SAT relationship. Finally, Fig. 3h reveals the difference in future SAM-SAT relationships between the two storylines (Storyline B–Storyline C). Future changes in Antarctic SAM-SAT correlations are predominantly more negative (positive) over the Peninsula and West Antarctica in Storyline B (Storyline C) with opposite relative changes over East Antarctica. Regions where the differences are

significant are Marie Byrd Land in West Antarctica (negative) and the eastern part of East Antarctica, from Terre Adélie to Oates Land and Wilkes Land, and parts of the Dronning Maud Land coast (positive).

The winter SAM structure for the two storylines and ERA5 is shown in Fig. 4. In the present we note that there are three regions where the storyline SAM structures are significantly different (Fig. 4a), located over South America (50–85°W), the south–east Atlantic Ocean (5°W clockwise to 20°E) and south of Australia (115–150°E). In the first of these, the longitude of maximum northward projecting negative correlation anomalies (hereinafter NPNCs) in both storylines is positioned east of that in ERA5, located in the south–west Atlantic rather than the ABS (south–east Pacific), with Storyline B being most different. The region of NPNCs in the ABS represents the primary asymmetrical component of the SAM in recent decades and is associated with El Niño-Southern Oscillation (ENSO) teleconnections (e.g., Campitelli et al. 2021). The reduced storyline NPNCs at these longitudes, especially in Storyline B, indicate that such teleconnections are underestimated in these storyline models, an attribute that is valid for CMIP6 models as a whole (Feng et al. 2024). Conversely, the region of NPNCs extending into the south–west Atlantic that is not present in the contemporaneous ERA5 data was observed in earlier data from the 1950s and 1960s (Marshall et al. 2022). In the two other regions with significant differences in SAM structure between the storylines, Storyline B has a SAM structure closest to ERA5.

There are fewer sectors of significant differences in SAM structure between the two models in the future (Fig. 4b). These are focused at 0°, where Storyline B has NPNCs while Storyline C has southward projecting positive correlation anomalies (SPPCs), and in the south–west Indian Ocean (20–50°E), where Storyline C has stronger NPNCs than Storyline B. In the ABS region both models have stronger NPNCs than in the present, perhaps indicative of ENSO

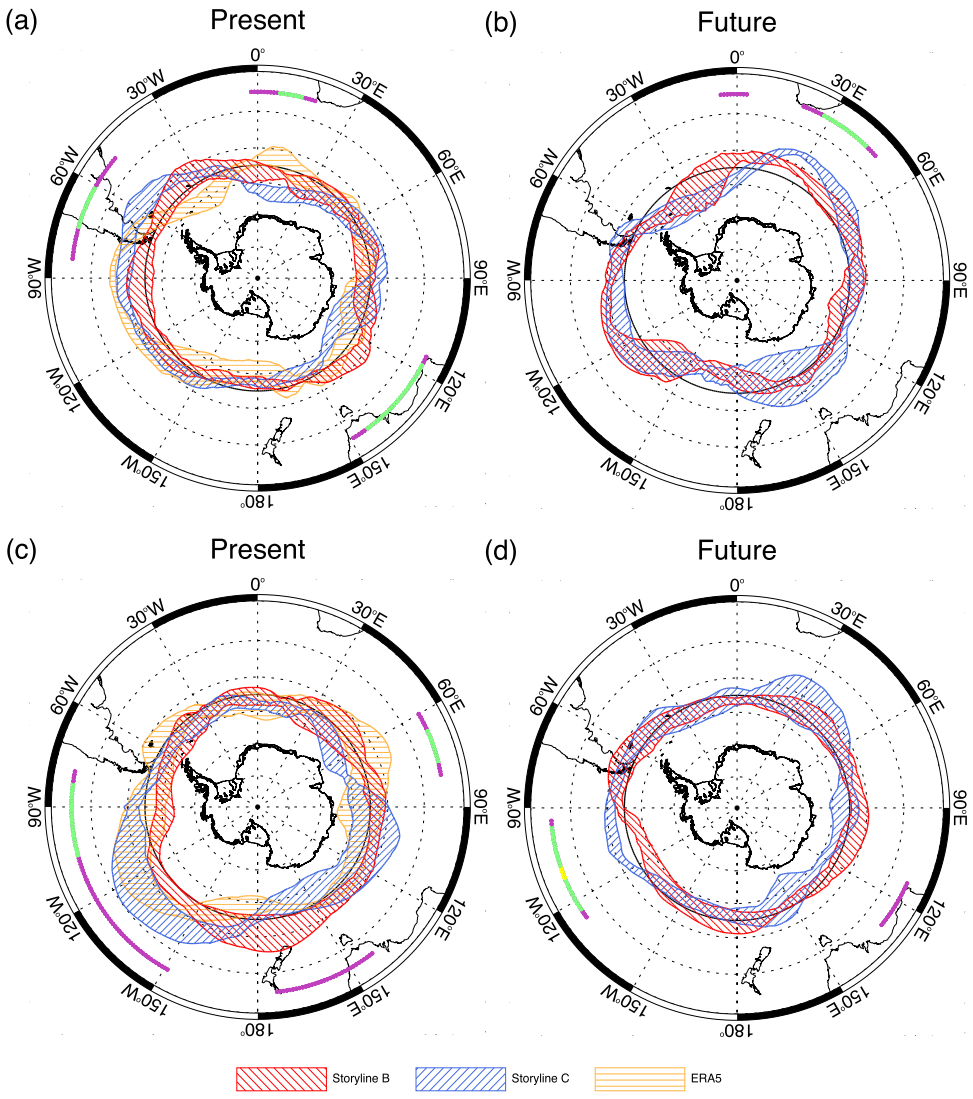

Fig. 4 Mean SAM structure based on decadal zonal SAM-SLP correlation anomalies at 55°S for the 30-year present and future periods, for winter (**a** and **b**) and summer (**c** and **d**). Storyline B is shown in red, Storyline C in blue and ERA5 in orange. The shading represents the interquartile range of the decadal zonal SAM-SLP correlation anomalies at that longitude. Positive (negative) values are plotted proportionately (in latitudinal degrees) south (north) of 55°S (black line). The dots at 35°S indicate the presence of a significant difference in the SAM-SLP correlation anomalies between Storylines B and C at that longitude: purple, green and yellow dots represent $p<0.10$, $p<0.05$ and $p<0.01$, respectively

teleconnections to the Antarctic becoming amplified in the future (McGregor et al. 2022).

To help quantify these model differences in winter SAM structure the zonal SAM-SLP correlation anomalies at 55°S are decomposed into the first four zonal wave numbers. The mean amplitude, phase and explained variance for each of these are given in Tables S2 and S3 for the present and future winter, respectively, and illustrated in Fig. 5. Testing for significance differences of these parameters between the two storylines was undertaken using decadal correlation anomalies but, due to the small number of independent samples, very few significant differences were found.

In the present only the amplitude of wave number 3 is significantly different, being higher in Storyline C, although not as high as in ERA5 (Table S2): thus, the explained variance by this wave number is much too low in both storylines. Focusing on the key region of NPNCs in the ABS, we observe that in ERA5 wave numbers 2–4 have correlation-anomaly minima in this region, whereas there are no minima in Storyline B and only for wave numbers 1 and 2 in Storyline C (Fig. 5a, c, e). In Storyline B wave numbers 1–3 have very small amplitudes such that the zonal flow associated with the SAM is too strong, as previously noted (Nan et al. 2019). While there is more 'waviness' in Storyline C, wave numbers 1 and 2 explain almost 80% of the variance, compared to ~50% in ERA5.

However, in the future, both wave numbers 2 and 3 become more evident in Storyline B, and the latter in Storyline C (Table S3), such that a region of NPNCs is located in the ABS in both storylines, broadly similar to ERA5 in the present (Fig. 4b). There are no significant differences in zonal wave number parameters between the two storylines in the future. In addition, in Storyline B there are sectors on either side of the ABS NPNCs that have correlation-anomaly maxima with all three nodes corresponding closely to wave number 3 (Fig. 5b). However, there are few areas of marked correlation-anomaly minima around East Antarctica, and thus the Storyline B SAM structure is predominantly zonal. In Storyline C there is slightly more variation in correlation-anomaly amplitude than in the present, so there is a significant difference between the two storylines centred at 30°E (cf. Figure 4b). Figure 5d indicates this region is associated with correlation-anomaly minima in wave numbers 3 and 4 in Storyline C.

Estimates of the meridional wind component associated with SAM+ integrated from the SAM structure (see Sect. 2.6) in the two storylines are shown for the present in Fig. S2a and future in Fig. S2b, respectively. A northerly (southerly) wind component is likely to lead to a more positive (negative) SAM-SAT relationship due to the advection of warm moist air from the extra-tropics (advection of cold dry air from the Antarctic continent). In the present period one of the primary differences between the storyline models occurs in the Peninsula region. In Storyline B, SAM+ is linked to southerlies in the western Weddell Sea, but in Storyline C it is associated with northerlies further east. Hence the 'standard' local positive SAM-SAT relationship in Storyline B is missing (Fig. 3a) but partially present in Storyline C (Fig. 3b). There are also clear differences between the storylines in Terre Adelie and Wilkes Land in East Antarctica:

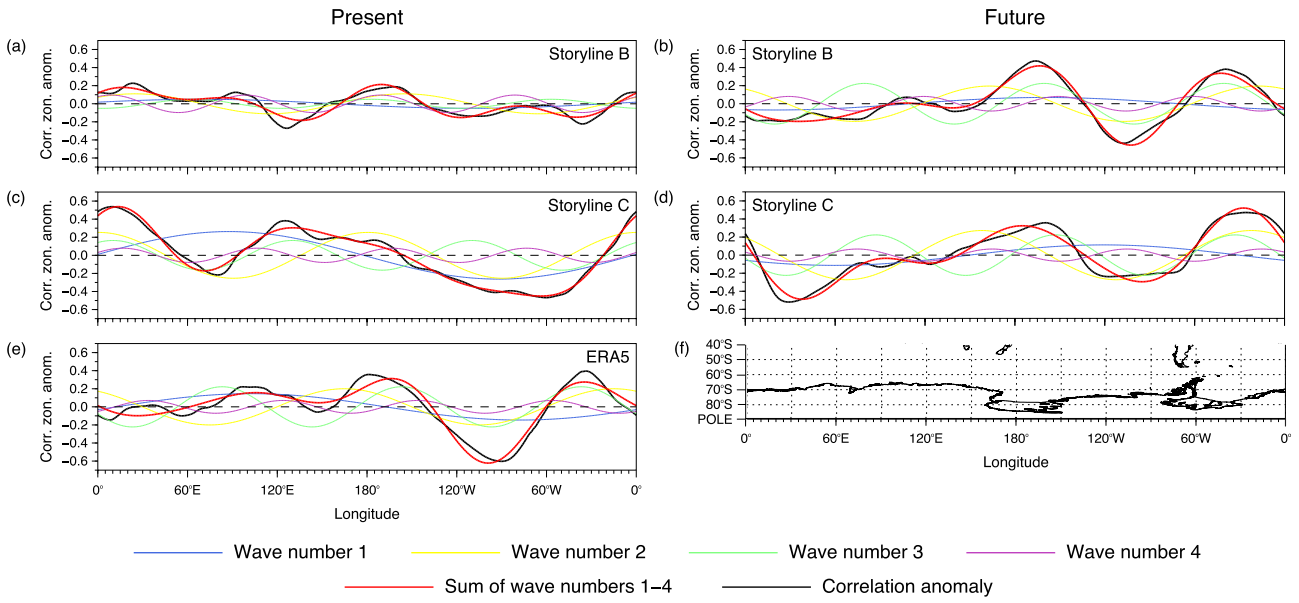

Fig. 5 The first four zonal waves computed from the winter zonal SAM-SLP correlation anomalies at 55°S. Storyline B, **a** the present and **b** the future; Storyline C, **c** present and **d** future and ERA5, **e** present, **f** reference coastline map of Antarctica. Wave numbers 1–4 are shown in blue, yellow, green and purple, respectively. The thick black and red lines represent the actual correlation anomaly and the sum of the first four zonal wave numbers, respectively

in Storyline B, SAM+ is associated with southerlies in the former region and strong northerlies in the latter, while the meridional wind components are opposite in Storyline C (Fig. S2a).

Figure S2b indicates greater differences in the longitudinal variability of the meridional wind related to SAM+ between storylines in the future period than the present. Nonetheless, the Peninsula is one region of greater similarity with both storylines having northerlies associated with SAM+ and thus both have positive regional SAM-SAT correlations in this period (see Fig. 3d and e). Around East Antarctica, Storyline B has strong southerlies between 0–30°W while Storyline C has a similar feature at 10°W clockwise to 30°E. Although Table S3 indicates no marked differences in the phase of any of the wave numbers between the two storylines, Fig. 5b and d indicate that the longitude of these northerlies is especially related to zonal wave numbers 2 and 3. The prominent changes in SAM structure in both storylines in the Amundsen Sea region (Fig. 4b) leads to a sector of strong southerlies off West Antarctica associated with SAM+ (Fig. S2b): thus, there are small areas of Marie Byrd Land where the negative SAM-SAT relationship becomes significant, which were not present in either storyline during the present (see Fig. 3a, b, d and e).

3.1.2 Summer

For summer, Storylines B and C are represented by CESM2-WACCM and MPI-ESM1-2-LR, respectively (Table 2). Simpson et al. (2020) observed that the CESM2 models, including those with the WACCM component as employed here, were able to characterise the general structure of the SAM well but were less good at representing the zonal asymmetries, including the principal region of NPNCs in the ABS. As mentioned previously, the SAM structure is also too zonal in MPI-ESM1-2-LR (Coburn and Pryor 2021).

The population of summer SAM values for the two storylines across the present and future periods is shown in Fig. 2c and d, respectively. In the present both have similar distributions to each other and, especially Storyline B, to ERA5. Similar to winter, the SAM Index in both summer storylines is projected to become significantly more positive in the future and also the storyline SAM Indices become significantly different ($p<0.01$) from each other. Again, Storyline C, associated with a longer delay in SPV breakdown (and thus a stronger SPV in the lead up), has a more positive SAM than Storyline B, despite CESM2-WACCM having a greater future warming than MPI-ESM1-2-LR (Table 2), and its distribution is negatively skewed, similar to Storyline C in winter. We note that the typical future SAM values are projected to be lower in summer than winter relative to the present and the range of values is markedly smaller (see Fig. 2), likely a result of ozone recovery that will partially counteract the effects of GHG increases in this season.

The summer SAM-SAT correlations and correlation-differences are shown in Fig. 6. Both storyline models reproduce a region of positive SAM-SAT correlations over the Peninsula in the present (see Figs. 6a, b) although it is very weak in Storyline C. While in both cases this is smaller in extent and magnitude than in ERA5, some station observations indicate that the relationship may actually be too positive in the reanalysis: there is a weak negative SAM-SAT correlation at Vernadsky on the western side of the Peninsula and the magnitude of the positive correlation at Orcadas, in the South Orkney Islands, is much smaller than in ERA5 (Fig. 6c). The spatial pattern of negative correlations across almost all the remainder of the continent is portrayed accurately in both models. However, the proportion that has a statistically significant SAM-SAT relationship differs markedly. In the Storyline B model almost the entirety of both West and East Antarctica has a significant negative relationship and the region where $r_{max}<-0.6$ is far greater, whereas in Storyline C and ERA5 the region of significance is largely restricted to East Antarctica between 75 and 170°E. Station observations reveal that summer SAT is not significantly correlated with the SAM at any of the Antarctic Plateau stations across the same period (see Fig. 6c). Therefore, the 'real' extent of the region of significance is likely much closer to that indicated by Storyline C than Storyline B. However, there is a small area of positive correlation in coastal Enderby Land in the Storyline C model that is not present in ERA5 or observations: indeed, Syowa station, located in this region, actually has a significant negative SAM-SAT correlation (Fig. 6c).

The future period demonstrates markedly different extents in the positive SAM-SAT relationship in the Antarctic Peninsula between the two storylines (Fig. 6d and e), with a much smaller area in Storyline B than Storyline C: the former is limited to the eastern coast while the latter encompasses all the northern half of the Peninsula. Given the broadly comparable regional SAM-SAT patterns in the present period, the storylines have opposite impacts on the SAM-SAT relationship in the Peninsula (Fig. 6f and g), although the temporal differences in both cases are not statistically significant. These changes extend from the Peninsula through Ellsworth Land, the Filchner–Ronne Ice Shelf and across much of West Antarctica. In Storyline B, some of the changes to more negative SAM-SAT correlations in this region are significant (Fig. 6f) while the changes to less negative correlations in Storyline C are not (Fig. 6g). Interestingly, while the SAM-SAT relationship remains negative across East Antarctica in the future (Fig. 6d and e), temporal changes in the sign of the SAM-SAT relationship

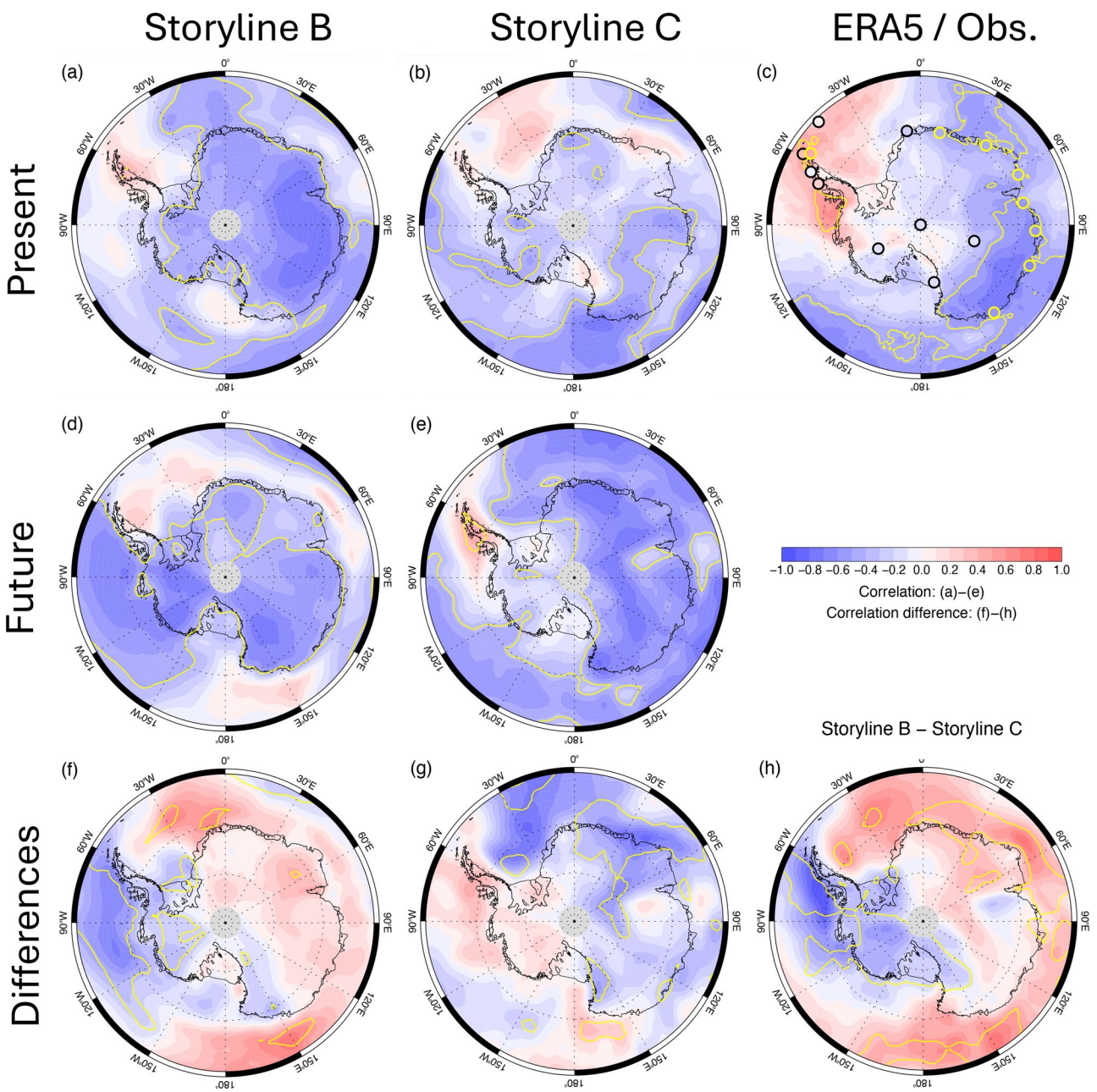

Fig. 6 As Fig. 3 for summer

are opposite to those in the Peninsula and West Antarctica in both storylines (Fig. 6f, g and h): in Storyline B (Storyline C) the future generally has weaker (stronger) negative SAM-SAT correlations than the present (Fig. 6f and g). In both storylines there are small areas of East Antarctica where these changes are significant, but most notably in Dronning Maud Land–Enderby Land and Victoria Land in Storyline C (Fig. 6g).

Figure 6h demonstrates that storyline differences in the future Antarctic SAM-SAT relationship are generally greater for summer than in winter (see Fig. 3h). During summer, Storyline B has more negative SAM-SAT correlations across the Peninsula, West Antarctica and both the Filchner–Ronne and Ross Ice Shelves than Storyline C. For most of West Antarctica and the Ross Ice Shelf extending into southern Victoria Land, these differences are statistically significant. While this is not the case over the Peninsula itself, the Bellingshausen Sea, immediately to the west, is the area with the largest correlation difference (>0.9) south of 60°S (Fig. 6h). In contrast, Storyline B has weaker negative correlations across much of the Southern Ocean except the ABS with several areas significantly different to

Storyline C. For East Antarctica there is a mix of positive and negative differences in SAM-SAT correlations between the storylines. The differences are statistically significant in Victoria Land (Storyline B more negative) and parts of Dronning Maud Land and Enderby Land (Storyline B more positive) (Fig. 6h).

The SAM structure and zonal wave numbers for the summer are shown in Figs. 4c, d and 7, respectively. In addition to Fig. 4c, comparison of the zonal wave numbers (see Table S4 and Fig. 7a) demonstrates that the SAM structure is far too zonal in the Storyline B model in the present, in agreement with Simpson et al. (2020), with wave 1 explaining ~76% of the total variance (the equivalent value for ERA5 is 9%). Furthermore, the amplitude of the first three wave numbers is significantly larger in Storyline C. This is the primary reason why there are three sectors where the SAM structure is significantly different between the two storylines (see Fig. 4c). The largest of these is in the south-east Pacific, where ERA5 has a region of significant NPNCs: these are very well reproduced in Storyline C but almost absent in Storyline B. Thus, like the majority of CMIP6 models, CESM2-WACCM is unable to correctly reproduce the primary SH extratropical teleconnection (Feng et al. 2024), whereas in contrast the MPI-ESM1-2-LR model does especially well here. Examining Table S4, it is apparent that, although the relative explained variance of the first three wave numbers is quite different between Storyline C and ERA5, their phases are remarkably similar such that the region of maximum NPNCs are located at the correct longitude (see Fig. 7c and e). Interestingly, while there is a small longitudinal shift in the local northerly winds associated with SAM+ between the two storylines, with maxima at 85° and 105°W (Fig. S2a) this does not translate into a significantly better reproduction of the positive SAM-SAT relationship in the Peninsula. This may be because of a lack of secondary NPNCs in the south-west Atlantic at ~45°W (similar to both storyline models in winter: see Fig. 4a) that is present in ERA5 but not in Storyline C (Fig. 4c).

Elsewhere in the present, between 150 and 180°E Storyline B does have a region of NPNCs while Storyline C actually has SPPCs: the slightly positive ERA5 SAM-SLP correlation anomalies are more similar to the latter (Fig. 4c). This difference in longitude between the main region of NPNCs of the two storylines is predominantly associated with changes in the location of the ASL and is discussed further in Sect. 3.2.2. This sector (80–120°W) is also where the principal difference in meridional winds linked to the SAM is found (Fig. S2a), as it lies on opposite sides of the maximum NPNCs in the two models. In Storyline C, SAM+ is associated with a strong southerly component while for Storyline B the equivalent wind component is more variable (Fig. S2a). However, this contrast does not convert into any marked difference in regional SAM-SAT correlations between the two storylines (see Fig. 6a and b). The other region of significant difference in SAM structure is between 60 and 80°E, where Storyline C incorrectly has SPPCs in contrast to ERA5 (Fig. 4c). This difference may explain the small area of positive SAM-SAT correlations at these longitudes in this storyline (see Fig. 6b).

For the future period, the wave-number data indicate that the SAM structure in the two storyline models is actually closer in the future than the present, with only the phase and variance explained by wave number 2 being significantly different (Table S5). In particular, the SAM structure in

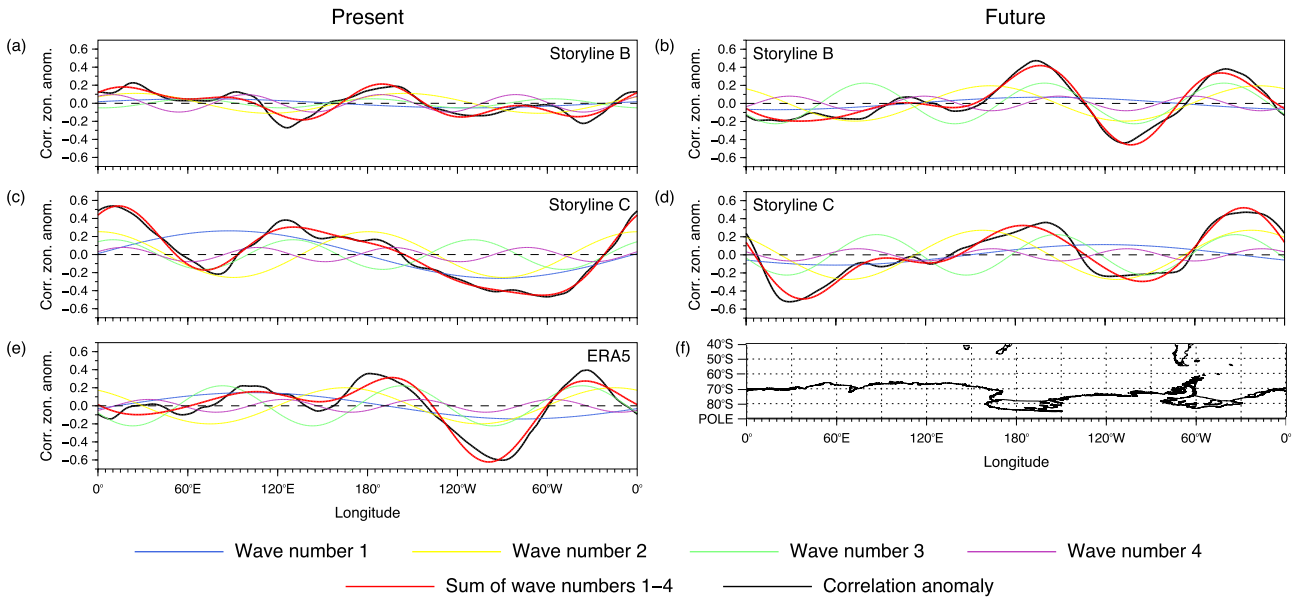

Fig. 7 As Fig. 5 for summer

Storyline C has become more zonal (see Fig. 7c and d), with a decreased amplitude of the first four wave numbers compared to the present. Nevertheless, the SAM structure of the two storylines remains significantly different in the region of the ABS despite both storylines having more positive SAM-SAT anomalies in this sector (90–150°W): in Storyline B there are now SPPCs whereas in Storyline C the magnitude of the NPNCs is markedly reduced. The location of the latter has also shifted east by ~40°, while the principal region of NPNCs in Storyline B is unchanged, centred at ~180° (see Fig. 4c and d). However, another area of NPNCs is also present in Storyline B at 30–90°W. The largest meridional wind component—a northerly—associated with SAM+ in this storyline is located on the western flank of this feature at 90°W and a similar magnitude wind component is situated at 120°W in Storyline C (Fig. S2b). Thus, the offshore cold airflow is markedly closer to the Antarctic Peninsula in Storyline B than Storyline C leading to the lack (presence) of a positive SAM-SAT west of the Peninsula in the former (latter) (see Fig. 6d and e). The second region of significant difference in SAM structure is at ~120°E with Storyline B (Storyline C) having weak NPNCs (SPPCs). However, this does not lead to any marked difference in the local meridional flow associated with SAM+ (Fig. S2b) or SAM-SAT correlation. Therefore, as noted above, significant storyline differences in SAM-SAT correlation resulting from variations in SAM structure are predominantly limited to West Antarctica (see Fig. 6h).

3.2 The strength and location of the Amundsen Sea Low (ASL)

3.2.1 Winter

For winter in the present the median relative depth of the ASL in ERA5 is 9 hPa, with both storylines having values about ~1 hPa less (Fig. 8a). In terms of ASL longitude, Storyline B is significantly different to ERA5 ($p<0.10$), being typically too far east by ~15° (Fig. 8b), a characteristic shared by some earlier CMIP5 models (Hosking et al. 2013). In addition, the distribution of longitudes is also less positively skewed than the reanalysis. While the median longitude in Storyline C is closer to ERA5, the interquartile range is significantly greater, with the ASL more frequently located further east than either the reanalysis or Storyline B (Fig. 8b). Thus, it appears likely that it is this positional change that is primarily responsible for the significant difference in SAM structure east of the ASL (50–85°W) (Fig. 4a).

In the future the winter ASL median relative depth in Storyline C is comparatively unchanged whereas in Storyline B it declines such that the median value is 1 hPa lower than at present. In Storyline C the interquartile range of relative depth has increased but the overall range is reduced, with a decrease in the maximum value. Future changes in the median ASL longitude comprise relatively small easterly shifts for both storylines. Both storylines have an increase in longitudinal variability, but the distributions are negatively (positively) skewed for Storyline B (Storyline C). Thus, in the future, under Storyline B there will be a weaker winter ASL closer to the ABS whereas in Storyline C it will be stronger and positioned nearer to the Ross Sea. However, these differences are relatively small, as indicated by the lack of significant regional differences in SAM structure between the storylines (Fig. 4b), comparable local meridional wind components associated with SAM+ (Fig. S2b) and similar SAM-SAT relationships in the Peninsula region (Fig. 3h).

3.2.2 Summer

For summer, the relative depth of the ASL in the present period in Storyline C is also closer to ERA5 than Storyline B (Fig. 8c). The latter has an ASL ~1 hPa deeper compared to ERA5, perhaps surprising given that the SAM is known to be too zonal in CESM2-WACCM (Simpson et al. 2020). The result is a significant difference in relative depth between the storyline models ($p<0.10$). However, despite the use of different storyline B models for the two seasons, both storylines correctly have a weaker ASL in summer than winter in the present. Additionally, ERA5 demonstrates a markedly greater interannual variability in ASL longitude in summer than winter, as indicated by the interquartile range (see Fig. 8b and d). Storyline B has a median longitude closer to ERA5 but Storyline C better exhibits this greater variability. However, in the latter model the median location is significantly further west than ERA5: 153°W versus 115°W. Observations have shown that in summer the ASL is positioned closest to the Peninsula. Nevertheless, Storyline C correctly reproduces the NPNCs associated with the ASL better than Storyline B, if slightly too far west (Fig. 4c), likely because there is sometimes a secondary low closer to the location of the observed ASL (not shown).

In the future period there is a greater difference between summer ASL relative depth between storylines than the present, with Storyline B having a deeper ASL ($p<0.01$). There are no significant changes from present but the ASL in Storyline B becomes deeper, even though the SAM polarity is more positive than in the present so the overall hemispheric westerly flow might be expected to be stronger, and Storyline C has a shallower ASL on average. Regarding the ASL longitude, the difference between the two storylines is significant ($p<0.01$) and the interquartile ranges barely overlap in the future (Fig. 8d). Interestingly, the overall range among the two storylines is not that different but

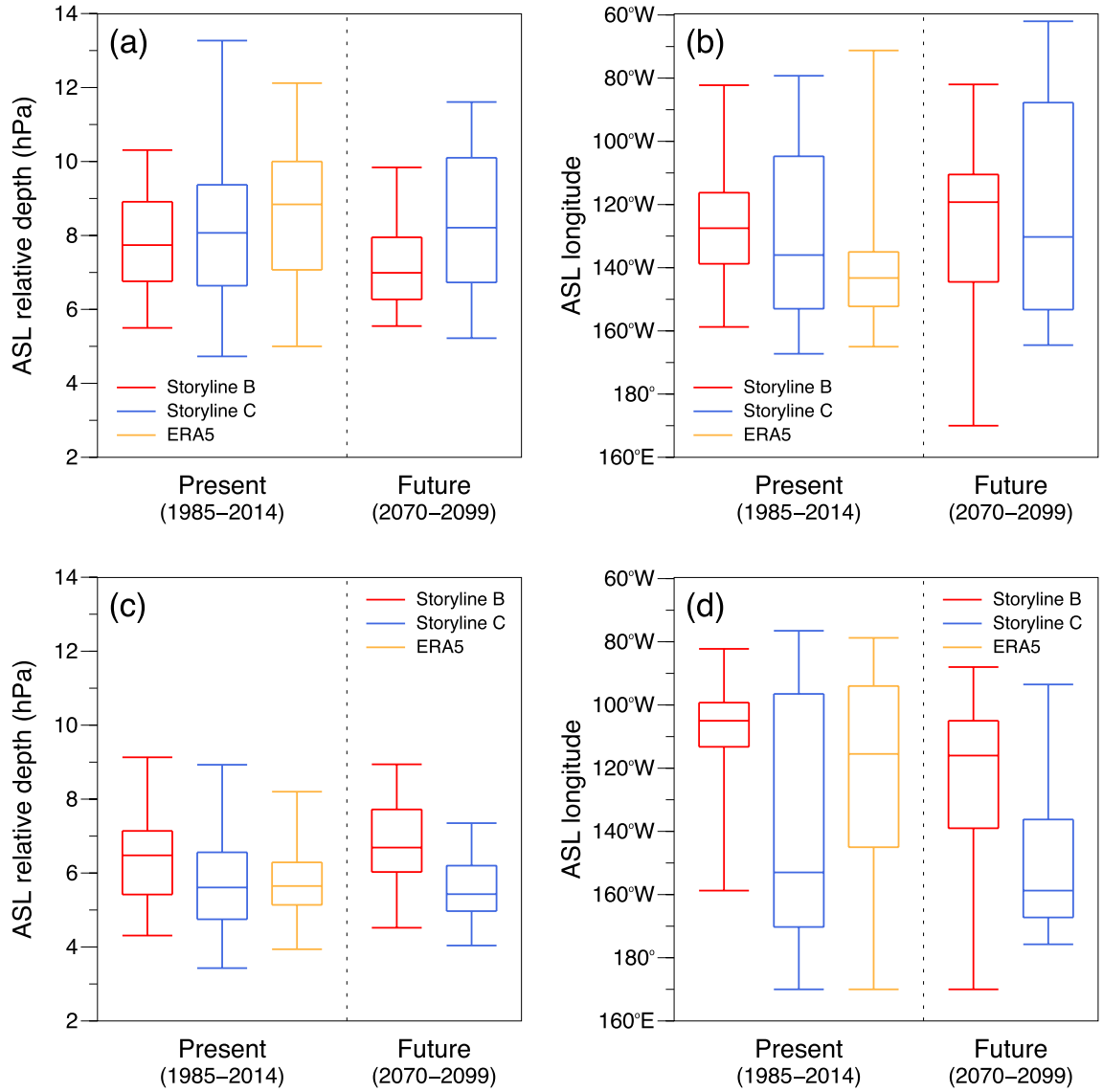

Fig. 8 ASL relative depth and longitude distributions for the present and future periods, for winter (**a** and **b**) and summer (**c** and **d**). Storyline B is shown in red, Storyline C in blue and ERA5 in orange. The median, upper and lower quartiles (boxes) and range (whiskers) are shown

Storyline B (Storyline C) is heavily negatively (positively) skewed. Thus, in the future in Storyline B a deeper ASL situated at ~105°W would mean enhanced northerly flow of warm maritime air into the Antarctic Peninsula, whereas in Storyline C, a weaker ASL to the west (~160°W) will favour inflow into West Antarctica. This prominent difference in the summer projections of the ASL between the storylines is apparent as the region of significant difference in SAM structure (Fig. 4d), the zonal shift in the regional northerly flow associated with SAM+ (Fig. S2b) and also significant differences in the SAM-SAT relationship in the West Antarctic-Peninsula sectors of Antarctica (Fig. 6h). Of course, given the incorrect location of the ASL in Storyline C in the present period, these projected future differences between summer storylines need to be treated with a measure of caution.

4 Discussion and conclusions

Here, we employ a storyline approach to examine possible future changes in the relationship between the SAM and Antarctic temperatures as a response to plausible physical changes in remote drivers of the SH high latitude atmospheric circulation according to the SSP5-8.5 projection. Specifically, we build on results from Williams et al. (2024), who used differences in the amount of SIE loss and either wintertime SPV strengthening or summertime SPV breakdown timing as drivers to derive four storylines of future

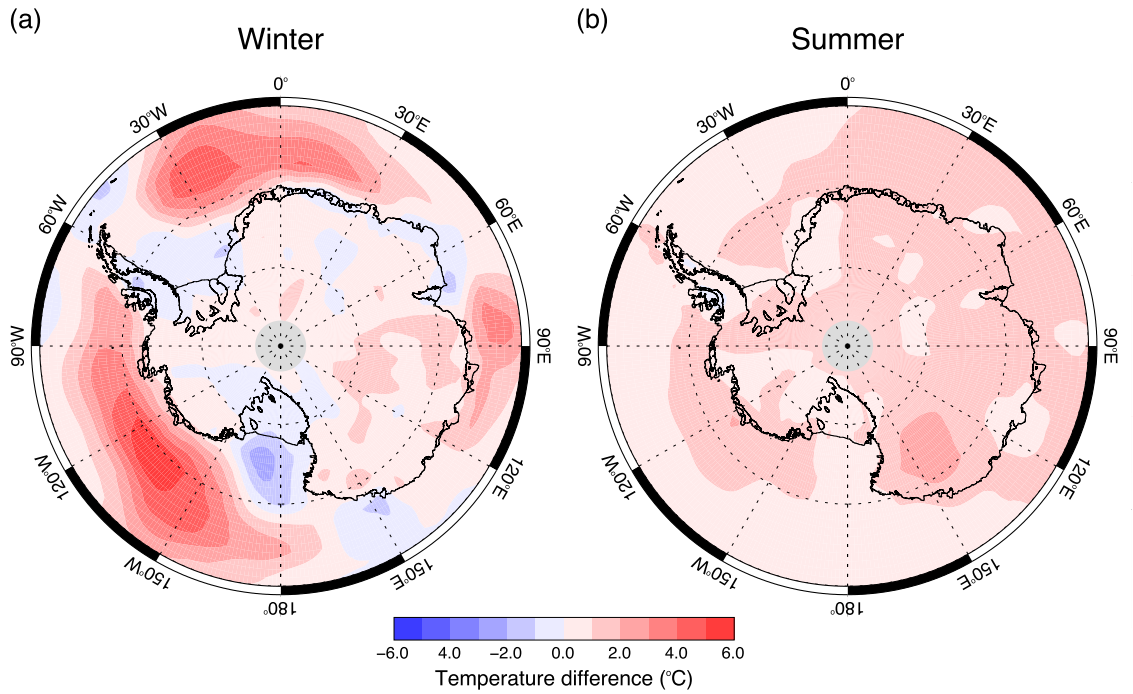

Fig. 9 SAT difference between future and present periods (Storyline B_{FUTURE}–Storyline $B_{PRESENT}$)–(Storyline C_{FUTURE}–Storyline $C_{PRESENT}$): **a** winter and **b** summer. The future SAT of the Storyline B models has been normalised to the Storyline C model future warming (see Table 2)

Antarctic climate change. We utilise two of their storylines, Storyline B and Storyline C, which represent future scenarios with high SIE loss and weak SPV and low SIE loss and strong SPV, respectively (see Table 1). Our results are based on individual CMIP6 models that Williams et al. (2024) selected as best representing these storylines in winter and summer. Despite there being a quality control component in this selection process, we find that the varying ability of these models to correctly reproduce the present SAM-SAT relationship across Antarctica may compromise the robustness of some of the projected changes. In particular, like the majority of CMIP6 models (e.g., Coburn and Pryor 2021), in most of the chosen models the SAM is too zonal and/or the principal non-annular component of the SAM in the ABS is located at the wrong longitude. This means that the meridional wind anomalies associated with the SAM are also incorrectly positioned. Similar issues were previously observed in many CMIP5 models (Marshall and Bracegirdle 2015). Nevertheless, the storyline models generally do well at reproducing the negative SAM-SAT pattern in East Antarctica (Figs. 3a, b and 6a, b) and, moreover, analysing projected changes in the patterns provides information about the likely direction that future SAM-SAT relationships will take.

Focussing initially on winter, there are few significant differences in the projected SAM-SAT relationship, despite there being greater differences in SAM structure and associated meridional wind components between the two storyline models in the future compared to the present. We also note that there is relatively little difference in actual SAT change between the pair of winter storylines over the Antarctic continent. Unsurprisingly, given that a significant difference in sea ice loss is a definition of storyline pair B and C, the largest SAT changes are situated over the Southern Ocean (Fig. 9a). Both storylines have a more positive SAM-SAT relationship over the Peninsula and West Antarctica (less negative) in the future, becoming more similar to ERA5 in the present, especially Storyline B (Fig. 3h). Another feature common to both future winter storylines is that SAT in the Dronning Maud Land region has a significantly more negative correlation with the SAM than at present, thus creating a stronger SAM-SAT dipole between the Peninsula and this region of East Antarctica (compare Fig. 3a, b, with Fig. 3d, e). This dipole corresponds to similar meridional winds associated with SAM+ in the two storyline models, both having northerlies in the Weddell Sea sector and southerlies in the ABS (Fig. S2b). Regions where there are significant SAM-SAT differences in the future are Marie Byrd Land in West Antarctica (Storyline B more negative) and the eastern part of East Antarctica, from Terre Adélie to Oates Land and Wilkes Land (Storyline B less negative) (Fig. 3h). As both models have similar regional SAM-SAT correlation values to ERA5 in these regions in the present, this divergence between the storylines may be considered relatively robust. In the future, a stronger winter ASL occurs closer to the Peninsula in Storyline B while in Storyline C it is weaker

and positioned nearer the Ross Sea (Fig. 8b and d). However, this does not translate into significant differences in the regional SAM-SAT relationship between the two storylines, perhaps indicating a lesser role for the ASL in governing the future winter climate of West Antarctica and the Peninsula.

In summer, the spatial SAM-SAT relationship across Antarctica in the storyline models generally better matches ERA5 in the present than those used in winter (Figs. 6a–c and 3a–c). While both summer models demonstrate a reduced extent and magnitude of positive SAM-SAT relationship over the Peninsula, station observations suggest this area is actually too pronounced in the reanalysis (Fig. 3a–c). In contrast to winter, the changes between present and future SAM-SAT in the summer storylines reveals differences of opposite sign across much of the Antarctic continent (Fig. 6f, g). For Storyline B, SAM-SAT correlations become more negative across the Peninsula, West Antarctica and both the Filchner–Ronne and Ross Ice Shelves whereas in Storyline C the opposite is projected to occur. For much of this region, these differences are statistically significant. Thus, the greater SAT changes in Storyline B than Storyline C are generally reduced in this region compared to East Antarctica (Fig. 9b). The Bellingshausen Sea is the area with the largest difference in correlation (< -0.9) south of 60°S (Fig. 6h). Across East Antarctica there is a mix of positive and negative differences in SAM-SAT correlations between the future storylines, some of which are significant. The future summer Storyline B ASL becomes deeper and is typically located at ~105°W, meaning enhanced northerly flow of warm maritime air into the Antarctic Peninsula, whereas in Storyline C, a weaker ASL to the west (~160°W) will favour inflow into West Antarctica (Fig. 8d). This prominent difference in the summer projections of the ASL between the storylines is apparent as a region of significant difference in SAM structure and a zonal shift in the sector of northerly flow associated with SAM+, and is responsible for the significant differences in SAM-SAT relationship in the West Antarctic-Peninsula regions of Antarctica (Figs. 6d, e, 4d and S2).

In this work we have demonstrated the potential for a clear divergence in future Antarctic SAM-SAT relationships between two physically plausible storylines, linked to variations in projected changes in Antarctic sea-ice extent and SPV strength: these distinctions are shown to be markedly greater in summer than winter, with significant differences across much of Antarctica in the former season.

This may be because the two storyline predictors explain up to 70% of midlatitude jet variance in summer compared to only 35% in winter (Williams et al. 2024). Of interest is the clear spatial pattern to these differences in summer: in Storyline B there is a more negative relationship between the SAM and SAT across the Peninsula and West Antarctica and a less negative one in East Antarctica and vice versa for Storyline C. Thus, given the general increase in the frequency of positive SAM polarity in both storylines (Fig. 2b), we might expect Storyline B to lead to less (greater) surface melt in the Peninsula and West Antarctica (East Antarctica) compared to Storyline C, with potentially significant impacts on the stability of the buttressing ice shelves in each region (e.g., Gilbert and Kittel 2021. The implication is that the differences between the spatial SAM-SAT relationship in the chosen pair of storylines have, in addition to repercussions for Antarctic ecosystems (e.g., Colesie et al. 2023; Schofield et al. 2024) via regional SAT changes, the potential to impact the rate of future global sea level rise.

We note here that, of course, SIE loss and SPV strengthening are unlikely to be the only drivers of the future SAM-SAT relationship and indeed the SAM itself is not the only influence on Antarctic SAT variability, with tropical SST variability known to have played an important role in driving recent Antarctic climate change (Li et al. 2021). However, given that many CMIP6 models struggle to correctly reproduce these tropical modes of variability (e.g., Coburn and Pryor 2021; Jacobson and Seager 2025), their influence on the SAM-SAT relationship has not been examined further here. A further caveat with this analysis is that based on a single model run for each storyline, we cannot fully determine the extent to which these projected future SAM-SAT changes are distinct from internal variability within the SH high latitude climate system. Therefore, we will expand the current work by employing single model initial-condition large ensembles to ascertain the importance of internal variability within the regional climate in driving the temporal variability of the SAM-SAT relationship in Antarctica.

Supplementary Information The online version contains supplementary material available at https://doi.org/10.1007/s00382-026-08081-8.

Acknowledgements This study was undertaken as part of the EU Horizon 2020 PolarRES project (https://polarres.eu/) and was funded under grant agreement number: 101003590. We thank the reviewers for their detailed comments and considered suggestions, which have significantly improved the clarity of the original manuscript.

Funding Horizon 2020 Framework Programme, 101003590.

Data availability The CMIP6 model data were obtained from the Earth System Grid Federation (ESGF). The specific data citations are: CAMS-CSM1-0 (historical): https://doi.org/10.22033/ESGF/CMIP6.9754. CAMS-CSM1-0 (SSP585): https://doi.org/10.22033/ESGF/CMIP6.11052. CESM2-WACCM (historical): https://doi.org/10.22033/ESGF/CMIP6.10071. CESM2-WACCM (SSP585): https://doi.org/10.22033/ESGF/CMIP6.10115. MPI-ESM1-2-LR (historical): https://doi.org/10.22033/ESGF/CMIP6.6595. MPI-ESM1-2-LR (SSP585): https://doi.org/10.22033/ESGF/CMIP6.6705. The SAT observations were obtained from https://legacy.bas.ac.uk/met/READER/data.html (doi: GB/NERC/BAS/PDC/00794); the SAT data for Byrd station from https://polarmet.osu.edu/datasets/Byrd_recon/byrd_temp_recon_mont

hly_revised_temp.txt; the ERA5 reanalysis data were acquired from the Copernicus Climate Data Store (CDS) https://cds.climate.copernicus.eu.

Declarations

Conflict of interest The authors have no relevant financial or non-financial interests to disclose.

References

Allen MR, Smith LA (1996) Monte Carlo SSA: detecting irregular oscillations in the presence of colored noise. J Clim 9:3373–3404

Arblaster JM, Meehl GA, Karoly DJ (2011) Future climate change in the southern hemisphere: competing effects of ozone and greenhouse gases. Geophys Res Lett 38:L02701. https://doi.org/10.1029/2010GL045384

Ayres HC, Screen JA, Blockley EW, Bracegirdle TJ (2022) The coupled atmosphere-ocean response to Antarctic sea ice loss. J Clim 35:4665–4685. https://doi.org/10.1175/JCLI-D-21-0918.1

Bozkurt D, Bromwich DH, Carrasco J, Hines KM, Maureira JC, Rondanelli R (2020) Recent near-surface temperature trends in the Antarctic Peninsula from observed, reanalysis and regional climate data. Adv Atmos Sci 37:477–493. https://doi.org/10.1007/s00376-020-9183-x

Bracegirdle TJ, Hyder P, Holmes CR (2018) CMIP5 diversity in southern westerly jet projections related to historical sea ice area: strong link to strengthening and weak link to shift. J Clim 31:195–211. https://doi.org/10.1195/JCLI-D-17-0320.1

Bracegirdle TJ, Holmes CR, Hosking JS, Marshall GJ, Osman M, Patterson M, Rackow T (2020) Improvements in circumpolar southern hemisphere extratropical atmospheric circulation in CMIP6 compared to CMIP5. Earth Space Sci 7:e2019EA001065. https://doi.org/10.1029/2019EA001065

Bromwich DH, Nicolas JP, Monaghan AJ, Lazzara MA, Keller LM, Weidner GA, Wilson AB (2013) Central west Antarctica among the most rapidly warming regions on Earth. Nat Geosci 6:139–145. https://doi.org/10.1038/NGEO1671

Bromwich DH, Nicolas JP, Monaghan AJ, Lazzara MA, Keller LM, Weidner GA, Wilson AB (2014) Correction: corrigendum: central west Antarctica among the most rapidly warming regions on Earth. Nat Geosci 7:76. https://doi.org/10.1038/NGEO2016

Bromwich DH, Ensign A, Wang S-H, Zou X (2024) Major artifacts in ERA5 2-m air temperature trends over Antarctica prior to and during the modern satellite era. Geophys Res Lett 51:e2024GL111907. https://doi.org/10.1029/2024GL111907

Byrne NJ, Shepherd TG, Polichtchouk I (2019) Subseasonal-toseasonal precitability of the southern hemisphere eddy-driven jet during austral spring and early summer. J Geophys Res Atmos 124:6841–6855. https://doi.org/10.1029/2018JD030173

Campitelli E, Diaz LB, Vera C (2022) Assessment of zonally symmetric and asymmetric components of the southern annular mode using a novel approach. Clim Dyn 58:161–178. https://doi.org/10.1007/s00382-021-05896-5

Ceppi P, Shepherd TG (2019) The role of the stratospheric polar vortex for the austral response to greenhouse gas forcing. Geophys Res Lett 46:6972–6979. https://doi.org/10.1029/2019GL082883

Clem KR, Renwick JA, McGregor J, Fogt RL (2016) The relative influence of ENSO and SAM on Antarctic Peninsula climate. J Geophys Res Atmos 121:9324–9341. https://doi.org/10.1002/2016JD025305

Coburn J, Pryor SC (2021) Differential credibility of climate modes in CMIP6. J Clim 34:8145–8164. https://doi.org/10.1775/JCLI-D-21-0359.1

Colesie C, Walshaw CV, Sancho LG, Davey MP, Gray A (2023) Antarctica's vegetation in a changing climate. Wires Clim Change 14:e810. https://doi.org/10.1002/wcc.810

Deng K, Azorin-Molina C, Yang S, Hu C, Zhang G, Minola L, Chen D (2022) Changes of southern hemisphere westerlies in the future warming climate. Atmos Res 270:106040. https://doi.org/10.1016/j.atmosres.2022.106040

Deser C, Phillips A, Bourdette V, Teng H (2012) Uncertainty in climate change projections: the role of internal variability. Clim Dyn 38:527–546. https://doi.org/10.1007/s00382-010-0977-x

Eyring V et al (2016) Overview of the Coupled Model Intercomparison Project Phase 6 (CMIP6) experimental design and organization. Geosci Model Dev 9:1937–1958. https://doi.org/10.5194/gmd-9-1937-2016

Feng Y, Screen JA, Hu X, Lin S, Williams NC, Yang S (2024) CMIP6 models underestimate ENSO teleconnections in the southern hemisphere. Geophys Res Lett 51:e2024GL110738. https://doi.org/10.1029/2024GL110738

Fogt RL, Marshall GJ (2020) The southern annular mode: variability, trends and climate impacts across the southern hemisphere. Wires Clim Change 11:e652. https://doi.org/10.1002/wcc.652

Fogt RL, Jones JM, Renwick J (2012) Seasonal zonal asymmetries in the southern annular mode and their impact on regional temperature anomalies. J Clim 25:6253–6270. https://doi.org/10.1775/JCLI-D-11-00474.1

Gettelman A et al (2019) The whole atmosphere community climate model version 6 (WACCM6). J Geophys Res Atmospheres 124:12380–12403. https://doi.org/10.1029/2019JD030943

Gilbert E, Kittel C (2021) Surface melt and runoff on Antarctic ice shelves at 1.5 °C, 2 °C and 4 °C of future warming. Geophys Res Lett 48:e2020GL091733. https://doi.org/10.1029/2020GL091733

Gilbert E, Orr A, Renfrew IA, King JC, Lachlan-Cope T (2022) A 20-year study of melt processes over Larsen C Ice Shelf using a high-resolution regional atmospheric model: 2. drivers of surface melting. J Geophys Res Atmos 127:e2021JD0360112. https://doi.org/10.1029/2021JD036012

Gong D, Wang S (1999) Definition of Antarctic oscillation index. Geophys Res Lett 26:459–462. https://doi.org/10.1029/1999GL900003

Gossart A, Helsen S, Lenaerts JTM, Vanden Broucke S, van Lipzig NPM, Souverijns N (2019) An evaluation of surface climatology in state-of-the-art reanalyses over the Antarctic ice sheet. J Clim 32:6899–6915. https://doi.org/10.1175/JCLI-D-19-0030.1

Goyal R, Jucker M, Sen Gupta A, Hendon HH, England MH (2021a) Zonal wave 3 pattern in the southern hemisphere generated by tropical convection. Nat Geosci 14:732–738. https://doi.org/10.1038/s41561-021-00811-3

Goyal R, Sen Gupta A, Jucker M, England MH (2021b) Historical and projected changes in the southern hemisphere surface westerlies.

Geophys Res Lett 48:e2020GL090849. https://doi.org/10.1029/2020GL090849
Hersbach H et al (2020) The ERA5 global reanalysis. Q J Royal Met Soc 146:1999–2019. https://doi.org/10.1002/qj.3803
Hosking JS, Orr A, Marshall GJ, Turner J, Phillips T (2013) The influence of the Amundsen–Bellingshausen seas low on the climate of west Antarctica and its representation in coupled climate model simulations. J Clim 26:6633–6648. https://doi.org/10.1175/JCLI-D-12-00813.1
IPCC (2023) Climate change 2023: Synthesis report. Contribution of working groups I, II and III to the sixth assessment report of the intergovernmental; panel on climate change [Core Writing Team, H Lee and J Romero (eds.)]. IPCC, Geneva, Switzerland, pp. 35–115 https://doi.org/10.59327/IPCC/AR6-9789291691647
Jacobson TW-P, Seager R (2025) Pacific decadal variability and its hydroclimate teleconnections in CMIP6 models. J Clim 38:5103–5127. https://doi.org/10.1175/JCLI-D-24-0616.1
Keeble J et al (2021) Evaluating stratospheric ozone and water vapour changes in CMIP6 models from 1850 to 2100. Atmos Chem Phys 21:5015–5061. https://doi.org/10.5194/acp-21-5015-2021
King JC, Marshall GJ, Colwell S, Arndt S, Allen-Sader C, Phillips T (2022) The performance of the ERA-Interim and ERA5 atmospheric reanalyses over Weddell Sea pack ice. J Geophys Res Oceans 127:e2022JC018805. https://doi.org/10.1029/2022JC018805
Knutti R, Massin D, Gettelman A (2013) Climate model genealogy: generation CMIP5 and how we got there. Geophys Res Lett 40:1194–1199. https://doi.org/10.1002/grl.50256
Li X et al (2021) Tropical teleconnection impacts on Antarctic climate changes. Nat Rev Earth Environ 2:680–698. https://doi.org/10.1038/s43017-021-00204-5
Marshall GJ (2007) Half-century seasonal relationships between the southern annular mode and Antarctic temperatures. Int J Climatol 27:373–383. https://doi.org/10.1002/joc.1407
Marshall GJ, Bracegirdle TJ (2015) An examination of the relationship between the southern annular mode and Antarctic surface temperatures in the CMIP5 historical runs. Clim Dyn 45:1513–1535. https://doi.org/10.1007/s00382-014-2406-z
Marshall GJ, Thompson DWJ (2016) The signatures of large-scale patterns of atmospheric variability in Antarctic surface temperatures. J Geophys Res Atmos 121:3276–3289. https://doi.org/10.1002/2015JD024665
Marshall GJ, Orr A, Turner J (2013) A predominant reversal in the relationship between the SAM and east Antarctic temperatures during the twenty-first century. J Clim 26:5196–5204. https://doi.org/10.1175/JCLI-D-12-00671.1
Marshall GJ, Fogt RL, Turner J, Clem KR (2022) Can current reanalyses accurately portray changes in southern annular mode structure prior to 1979? Clim Dyn 59:3717–3740. https://doi.org/10.1007/s00382-022-06292-3
Mauritsen T et al (2019) Developments in the MPI-M earth system model version 1.2 (MPI-ESM1.2) and its response to increasing CO_2. J Adv Model Earth Syst 11:998–1038. https://doi.org/10.1029/2018MS001400
McGregor S, Cassou C, Kosaka Y, Phillips AS (2022) Projected ENSO teleconnection changes in CMIP6. Geophys Res Lett 49:e2021GL097511. https://doi.org/10.1029/GL2021097511
Mindlin J, Shepherd TG, Vera CS, Osman M, Zappa G, Lee RW, Hodges KI (2020) Storyline description of southern hemisphere midlatitude circulation and precipitation response to greenhouse gas forcing. Clim Dyn 54:4399–4421. https://doi.org/10.1007/s00382-020-05234-1
Morgenstern O (2021) The southern annular mode in 6th coupled model intercomparison project models. J Geophys Res Atmos 126:e2020JD034161. https://doi.org/10.1029/2020JD034161
Nan S, Yang J, Bao Y, Li J, Rong X (2019) Simulation of the northern and southern hemisphere annular modes by CAMS-CSM. J Met Res 33:934–948. https://doi.org/10.1007/s13351-019-8099-9
O'Neill BC et al (2016) The Scenario Model Intercomparison Projects (ScenarioMIP) for CMIP6. Geosci Model Dev 9:3461–3482. https://doi.org/10.5194/gmd-9-3461-2016
Orr A, Bracegirdle JJ, Hosking JS, Jung T, Haigh JD, Phillips T, Feng W (2012) Possible dynamical mechanisms for southern hemisphere climate change due to the ozone hole. J Atmos Sci 69:2917–2932. https://doi.org/10.1175/JAS-D-11-0210.1
Orr A et al (2023) Characteristics of surface 'melt potential' over Antarctic Ice Shelves based on regional atmospheric model simulations of summer air temperature extremes from 1979/80 to 2018/19. J Clim 36:3357–3383. https://doi.org/10.1175/JCLI-D-22-0386.1
Polvani LM, Waugh DW, Correa GJP, Son S-W (2011) Stratospheric ozone depletion: the main driver of twentieth-century atmospheric circulation changes in the southern hemisphere. J Clim 24:795–812. https://doi.org/10.1175/2010JCLI3772.1
Raphael MN et al (2016) The Amundsen Sea Low: variability, change and impact on Antarctic climate. Bull Amer Meteorol Soc 97:111–121. https://doi.org/10.1175/BAMS-D-14-00018.1
Rong XY et al (2019) Introduction of CAMS-CSM model and its participation in CMIP6. Clim Change Res 15:540–544. https://doi.org/10.12006/j.issn.1673-1719.2019.186
Saunderson D, Mackintosh AN, McCormack FS, Jones RS, van Dalum CT (2024) How does the southern annular mode control surface melt in east Antarctica. Geophys Res Lett 51:e2023GL105475. https://doi.org/10.1029/2023GL105475
Schofield O et al (2024) Antarctic pelagic ecosystems on a warming planet. Trends Ecol Evol 39:1141–1153. https://doi.org/10.1016/j.tree.2024.08.007
Shepherd TG (2014) Atmospheric circulation as a source of uncertainty in climate change projections. Nat Geosci 7:703–708. https://doi.org/10.1038/ngeo2253
Silvestri G, Vera C (2009) Nonstationary impacts of the southern annular mode on southern hemisphere climate. J Clim 22:6142–6148. https://doi.org/10.1175/2009JCLI3036.1
Simpkins GR, Karpechko AY (2012) Sensitivity of the southern annular mode to greenhouse gas emission scenarios. Clim Dyn 38:563–572. https://doi.org/10.1007/s00382-011-1121-2
Simpson IR et al (2020) An evaluation of the large-scale atmospheric circulation and its variability in CESM2 and other CMIP models. J Geophys Res Atmos 125:2020JD034161. https://doi.org/10.1029/2020JD034161
Soci C et al (2024) The ERA5 global reanalysis from 1940 to 2022. Q J R Meteorol Soc 150:4014–4048. https://doi.org/10.1002/qj.4803
Sui C, Yu L, Karpechko AY, Feng L, Liu S (2024) Influence of the Atlantic multidecadal oscillation and Interdecadal Pacific oscillation on Antarctic surface air temperature during 1900 to 2015. Acta Oceanol Sin 43:48–58. https://doi.org/10.1007/s13131-023-2247-x
Sun Y, Zhang Y, Wang Y, Heil P, Hou S, Zhai Z (2025) Constraining future Antarctic warming under five different emissions scenarios in the CMIP6 multi-models. Geophys Res Lett 52:e2024GL112662. https://doi.org/10.1029/2024GL112662
Taylor KE et al (2012) An overview of CMIP5 and the experiment design. Bull Amer Met Soc 90:485–498. https://doi.org/10.1175/BAMS-D-11-00094.1
Tewari K, Mishra SK, Salunke P, Dewan A (2022) Future projections of temperature and precipitation for Antarctica. Environ Res 17:014029. https://doi.org/10.1088/1748-9326/ac43e2
Thompson DWJ, Solomon S (2002) Interpretation of recent southern hemisphere climate change. Science 296:895–899. https://doi.org/10.1126/science.1069270

Thompson DWJ, Solomon S, Kushner PJ, England MH, Grise KM, Karoly DJ (2011) Signatures of the Antarctic ozone hole in southern hemisphere surface climate change. Nat Geosci 4:741–749. https://doi.org/10.1038/NGEO1296

Turner J, Marshall GJ, Clem K, Colwell S, Phillips T, Lu H (2020) Antarctic temperature variability and change from station data. Int J Climatol 40:2986–3007. https://doi.org/10.1002/joc.6378

van Vuuren DP et al (2011) The representative concentration pathways: an overview. Clim Change 109:5. https://doi.org/10.1007/s10584-011-0148-z

Wachter P, Beck C, Philipp A, Höppner K, Jacobeit J (2020) Spatio-temporal variability in the southern annular mode and its influence on Antarctic surface temperatures. J Geophys Res Atmos 125:e2020JD033818. https://doi.org/10.1029/2020JD033818

Wilks D (2016) The stippling shows statistically significant grid points: how research results are routinely overstated, overinterpreted, and what to do about it. Bull Amer Met Soc 97:2263–2273. https://doi.org/10.1175/BAMS-D-15-00267.1

Williams RS et al (2024) Future Antarctic climate: storylines of mid-latitude jet strengthening and shift emergent from CMIP6. J Clim 37:2157–2178. https://doi.org/10.1175/JCLI-D-23-0122.1

Zappa G, Shepherd TG (2017) Storylines of atmospheric circulation change for European regional climate impact assessment. J Clim 30:6561–6577. https://doi.org/10.1175/JCLI-D-16-0807.1

Zhang X et al (2022) Evaluation of the seasonality and spatial aspects of the southern annular mode in CMIP6 models. Int J Climatol 42:3820–3837. https://doi.org/10.1002/joc.7447

Zhang X, Wang Y, Hou S, Heil P (2023) Significant west Antarctic cooling in the past two decades driven by tropical Pacific forcing. Bull Amer Meteor Soc 104:1154–1165. https://doi.org/10.1175/BAMS-D-22-0153.2

Zhu J, Xie A, Qin X, Wang Y, Xu B, Wang Y (2021) An assessment of ERA5 reanalysis for Antarctic near-surface air temperature. Atmosphere 12:217. https://doi.org/10.3390/atmos12020217

Zou X et al (2023) Strong warming over the Antarctic Peninsula during combined atmospheric river and foehn events: contribution of shortwave radiation and turbulence. J Geophys Res Atmos 128:e2022JD038138. https://doi.org/10.1029/2022JD038138